Article

Analysis of retrackers' performances and water level retrieval over the Ebro River basin using Sentinel-3

Qi Gao [123,*], Eduardo Makhoul [1], Maria Jose Escorihuela [1], Mehrez Zribi [2], Pere Quintana Seguí [3], Pablo García [1] and Mònica Roca [1]

[1] isardSAT, Parc Tecnològic Barcelona Activa, Carrer de Marie Curie, 8, 08042 Barcelona, Catalunya; eduard.makhoul@isardsat.cat; mj.escorihuela@isardSAT.cat; pablo.garcia@isardsat.cat; monica.roca@isardsat.cat

[2] CESBIO (CNRS/CNES/UPS/IRD), 31401 Toulouse CEDEX 9, France; mehrez.zribi@ird.fr

[3] Observatori de l'Ebre (OE), Ramon Llull University, 43520 Roquetes, Spain; pquintana@obsebre.es

* Correspondence: qi.gao@ isardSAT.cat; Tel.: +34-933-505-508

Abstract: Satellite altimeters have been used to monitor river and reservoir water levels, from which water storage estimates can be derived. Inland water altimetry can therefore play an important role in continental water resource management. Traditionally, satellite altimeters were designed to monitor homogeneous surfaces such as oceans or ice sheets, resulting in a poor performance over small inland water bodies due to the contribution from land contamination in the returned waveforms. The advent of synthetic aperture radar (SAR) altimetry (with its improved along-track spatial resolution) has enabled the measurement of inland water levels with a better accuracy and an increased spatial resolution. This paper presents three specialized algorithms or retrackers to retrieve water levels from SAR altimeter data over inland water bodies dedicated to minimizing land contamination from the waveforms. The performances of the proposed waveform portion selection method with three retrackers, namely, the threshold retracker, Offset Centre of Gravity (OCOG) retracker and 2-step physical-based retracker, are compared. Time series of water levels are retrieved for water bodies in the Ebro River basin (Spain). The results show good agreement with in situ measurements from the Ebro Reservoir (width is approximately 1.8 km) and Ribarroja Reservoir (width is approximately 400 m) with un-biased root-mean-square errors (RMSEs) of approximately 0.28 m and 0.16 m, respectively. The performances of all three retrackers are also compared with the European Space Agency's ocean retracker in the Sentinel-3 Level-2 product.

Keywords: altimetry; retracking; Sentinel-3; synthetic aperture radar (SAR)

1. Introduction

Inland water systems constitute crucial resources of fresh water necessary for human survival. Water within rivers and reservoirs represents the primary supply of drinking water, agricultural irrigation and industrial water usage; it is also used to produce renewable hydrological energy. Consequently, with a decrease in the water level, the current dependence on non-renewable energy will increase, resulting in further pollution. In addition, floods that periodically occur in every region of the world represent threats to crops, settlements, infrastructure, and most importantly life. Therefore, it is important to monitor the water levels of inland water bodies to provide early-warning alerts for water shortages or flood predictions. Unfortunately, in situ gauging stations are not always available in many parts of the world, or they are otherwise not publicly available and are maintained by local authorities. However, thanks to satellite altimetry, we possess a powerful tool for monitoring the water levels both within inland water systems where no in situ data are available and within transboundary river basins.

Space-borne radar altimeters are essential tools for monitoring the oceans, a task they have performed for over 20 years [1]. Satellite altimeters have also proven to be valuable tools for monitoring the water levels within inland water systems, including lakes and rivers [2-4]. A list of satellite altimeters and their resolutions is shown in Table 1. Sentinel-3, the newest in-orbit satellite, has a temporal resolution of approximately 27 days and an inclination angle of approximately 98.6 degrees, which means that it can cover all Earth latitudes (i.e., the entire globe). Operating in high-resolution synthetic aperture radar (SAR) mode [5], the ground track separation at the equator is approximately 104 km, which is better than that (approximately 315 km) of the Jason satellite mission. Therefore, the ability to provide coverage of lakes and rivers is higher for Sentinel-3 than for Jason. In contrast, the CryoSat ground track separation at the equator reaches 7.7 km at the expense of its temporal resolution, which is 369 days. Sentinel-3 exhibits the best along-track resolution at 300 m, similar to the resolution of CryoSat in SAR and interferometric SAR (inSAR) modes. However, CryoSat focuses on the cryosphere and covers most continental surfaces in low-resolution mode (LRM). Therefore, Sentinel-3 constitutes the first altimeter mission that covers the globe completely in SAR mode and is thus the most ideal tool for inland water level monitoring that possesses a good global coverage and sufficient temporal and spatial resolutions.

Table 1. Satellite altimetry missions

Satellite mission	Mission period	Inclination	Revisit time	Along-track resolution	Ground track separation at equator
Geosat [1]	1985-1990	108 deg	17 days	1.7 km	164 km
ERS [2] 1 &2	1991-2011	98.5 deg	35 days	1.7 km (ocean mode) 3.4 km (ice mode)	80 km
TOPEX/Poseidon [3]	1992-2006	66 deg	10 days	2.3 km	315 km
GFO [4]	1998-2008	108 deg	17 days	1.7 km	164 km
Jason 1, 2, & 3	2001-present	66 deg	10 days	2.2 km	315 km
Envisat [5]	2002-2012	98.55 deg	30-35 days	1.7 km	80 km
CryoSat [6]	2010-present	92 deg	369 days	300 m (SAR & SARIN) 1.6 km (LRM)	7.7 km
HY-2 [7]	2011-present	99.3 deg	Two phases (14 days & 168 days)	1.9 km	100 km
SARAL [8]	2013-present	98.55 deg	35 days	1.4 km	75 km
Sentinel-3	2016-present	98.6 deg	27 days	300 m	104 km
CFOSAT [9]	2018-present	90 deg	13 days	1.4 km	165 km
SWOT [10]	Planned on 2021	77.6 deg	21 days	100 m	0
JASON-CS [11]/SENTINEL-6	Planned on 2022	66 deg	10 days	300 m	315 km

[1] Geodetic Satellite. [2] European remote sensing satellite. [3] Topography Experiment/Poseidon. [4] GEOSAT Follow-On satellite. [5] Environmental Satellite. [6] Earth Explorer Opportunity Mission. [7] Haiyang-2 / Ocean-2. [8] Satellite with Argos (Data Collection System) and ALtiKa (Altimeter in Ka-band). [9] Chinese-French Oceanography Satellite. [10] Surface Water Ocean Topography Mission. [11] Jason Continuity of Service Mission.

Most previous studies focused on relatively large water bodies with a scale of several kilometres. The first study that employed satellite altimetry for inland water bodies was performed by Koblinsky

et al. [6], who processed Geodetic Satellite (Geosat) waveforms to estimate the water levels at four sites in the Amazon basin. A root-mean-square error (RMS) of 70 cm was estimated between the satellite and in situ measurements. Since then, with new generations of satellites, the spatial resolution and the accuracy of the orbit determination have both increased, thereby increasing the accuracies of the estimation results. Accordingly, several studies focused on lakes and large rivers with scales ranging from more than 1000 km^2 to 80,000 km^2 and demonstrated good results [6-13]. For example, Nielsen et al. [11] used Environmental Satellite (Envisat) and CryoSat-2 SAR data to retrieve the water levels over Vaenern (Sweden, 5650 km^2) and Lake Okeechobee (Florida, 1900 km^2) and obtained very good accuracies with RMSEs varying from 4 cm to 9 cm between the satellite-retrieved water levels and in situ measurements. Currently, several online data hubs, such as the Database for Hydrological Time Series of Inland Waters (DAHITI) (https://dahiti.dgfi.tum.de/en/) [14], Rivers and Lakes (http://tethys.eaprs.cse.dmu.ac.uk/RiverLake/) [15], Hydroweb (http://hydroweb.theia-land.fr/) [16], Global Reservoir and Lake Monitoring (https://ipad.fas.usda.gov/cropexplorer/global_reservoir/) [17] and Thematic Exploitation Platform (TEP) for Hydrology (https://hydrology-tep.eo.esa.int/) [18], also provide time series of water levels over large lakes and rivers.

Numerous studies [19-23] have also focused on middle-sized water bodies. For example, Birkinshaw et al. [19] measured the Mekong River, the width of which varies from 400 m to 1700 m; their results showed RMSEs of approximately 44-65 cm for Envisat and 46-76 cm for European Remote-Sensing Satellite-2 (ERS-2). Da Silva et al. [20] studied water level time series over the Amazon River basin, which exhibits widths ranging from several kilometres to less than a hundred metres, using both Envisat and ERS-2; they showed a RMSE varying from 12 cm in the best cases to 40 cm in most cases and several metres in the worst cases. Furthermore, Michailovsky et al. [21] employed Envisat to monitor the Zambezi River basin and reported river widths reaching 80 m with RMSEs of 32-72 cm relative to in situ measurements at different locations. In addition, Maillard et al. [22] measured the water levels of medium-sized rivers with widths between 100 and 1000 m over the São Francisco River, Brazil, with RMSEs lower than 60 cm and better than 30 cm in some cases using Envisat and Satellite with ARgos and ALtiKa (SARAL) data. Clearly, most studies of middle-sized water bodies used mainly Envisat and ERS. In addition, most previous results referred to LRM altimeters, which provide accuracies on the order of tenths of centimeters. At present, with the launch of Sentinel-3 equipped with the SAR Altimeter (SRAL), which can eliminate sources of pollution that are found when using LRM altimetry for small objects [24], there is a need to evaluate these retrackers and their accuracies. Additionally, studies need to be performed to enrich the monitoring of middle-sized and small-sized water bodies. Therefore, one of our study objectives is to test the performance of Sentinel-3 over middle-sized and small-sized water bodies.

Since the remote sensing waveform depends on the surface reflecting the signal, altimeter data are usually applied by different retrackers adapted to different surfaces to better locate the height of the reflective surface. Well-developed retrackers have been developed for operation over the oceans and ice surfaces called ocean retrackers and ice retrackers, respectively; however, no retracker has been adapted for inland water bodies. Jarihani et al. [9] compared the results from different satellite missions for inland water bodies; most previous studies [9-12,20,22] used ice retrackers, and some others [9,10] included ocean retrackers. Nevertheless, different retrackers need to be developed and compared for inland water bodies.

In our study, we modelled three different retrackers, namely, the threshold retracker, the Offset Centre of Gravity (OCOG) retracker, and the 2-step physical-based retracker; the parameters of these retrackers were adjusted for inland water bodies, and they were applied directly over Sentinel-3 Level-1 data. Additionally, we attempted to limit land contamination within the received waveforms and to improve the accuracy for the monitoring of middle-sized and small-sized water bodies by including digital elevation model (DEM) information to select the waveform portion from nadir.

The remainder of this paper is organized as follows. In Section 2, the studied area and the database are presented. Section 3 introduces the methodologies, including the selection of the waveform portion, different retrackers and waveform filtering approach. Section 4 shows the

performances of the different retrackers and the results of the water level time series in comparison with the European Space Agency (ESA) Level-2 ocean retracked results and in situ measurements. Section 5 discusses the method and results. Finally, the conclusions are presented in Section 6.

2. Study area and database

2.1. Study area

Our study area encompasses the reservoirs and rivers in the Ebro River basin (Figure 1). The Ebro River, which has a length of approximately 928 km and a drainage basin with an area of approximately 85,550 km^2, is one of the most important rivers on the Iberian Peninsula [25]. The river flow is irregular throughout the year with low levels at the end of summer and high levels during the spring due to melt runoff in the Pyrenees, leading to a danger of flooding. The Ebro River is of great importance for agriculture in the summer, during which drought often occurs due to the continental Mediterranean climate. Nevertheless, the mean annual flow decreased by approximately 29% during the 20th century due to many causes: the construction of dams, the increasing demands for irrigation, and the evaporation (which is higher than the precipitation due to low rainfall amounts, high sunshine intensities and strong, dry winds) from reservoirs within the river basin [25].

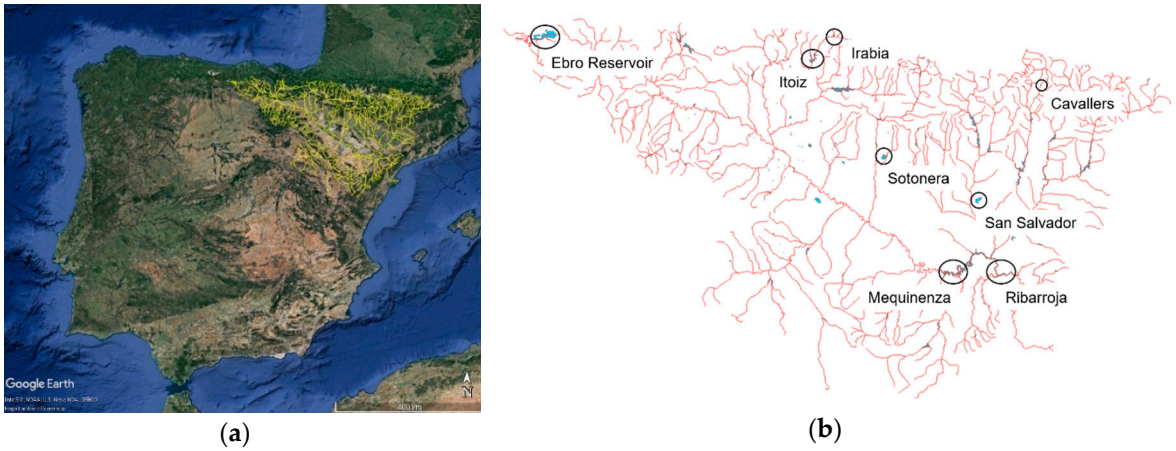

(**a**) (**b**)

Figure 1. The Ebro River basin: (**a**) the Ebro River network in the Iberian Peninsula; (**b**) the water bodies covered by Sentinel-3 satellite tracks with all available gauging stations.

The Pyrenees mountain range lies to the north of the Ebro River basin. As a consequence, it is challenging to retrieve the water surface heights of the studied area because the water bodies are relatively small and are greatly influenced by the mountainous terrain. The selected water bodies, for which we have gauging stations for validation, are shown in Figure 1. The coordinates, the widths of the water bodies covered with satellite tracks, and the approximate distances between the gauging station and satellite tracks are listed in Table 2.

Table 2. Selected water bodies

Water bodies	Coordinates	Width	Satellite tracks	Tracking mode	Gauging station distance
Ebro Reservoir	(43.0°N, 3.96°W)	1.8 km	014	Closed loop	8 km
Itoiz Reservoir	(42.81°N, 1.37°W)	400 m-2.7 km depends on satellite tracks	165	Closed loop	2 km
Irabia Reservoir	(42.99°N, 1.15°W)	130 m	186	Closed loop	450 m

Sotonera Reservoir	(42.12°N, 0.68°W)	4.5 km	222	Closed loop	1.5 km
Ribarroja Reservoir	(41.24°N, 0.40°E)	400 m	242	Open loop	3.5 km
Mequinenza Reservoir	(41.26°N, 0.04°W)	600 m	279	Open loop	30 km
Cavallers Reservoir	(42.59°N, 0.86°E)	800 m	299	Open loop	500 m
San Salvador Reservoir	(41.78°N, 0.20°E)	1.2 km	242	Open loop	2.5 km

2.2. Data base

2.2.1. Sentinel-3

Sentinel-3 is an ocean and land mission based on a constellation of two satellites (Sentinel-3A and Sentinel-3B). Sentinel-3A was launched on 16 February 2016 with data available beginning in June 2016 and was followed by Sentinel-3B, which was launched on 25 April 2018. The SRAL instrument is the main topographic sensor used to provide water level measurements, and hence, it is used in our research. The detailed parameters of the Sentinel-3 SRAL are listed in Table 3 [26].

Table 3. Parameters of the Sentinel-3 SRAL

Radar bands	**Ku** (13.575 GHz, bandwidth=350 MHz); C (5.41 GHz, bandwidth=320 MHz)
Radar measurement modes	**SAR** and LRM
Tracking modes	Closed and open loop
Pulse repetition frequency	17.8 KHz (SAR), 1.9 KHz (LRM)
Total range error	3 cm
Altimetry data products	Level-0, **Level-1**, Level-2 Near real-time (NRT), short-time critical (STC), and **non-time critical (NTC)**

To acquire altimeter measurements, the Sentinel-3 SRAL transmits pulses at a Ku-band frequency, which is complemented by a C-band frequency to correct range delay errors due to the varying density of electrons in the ionosphere [26]. Sentinel-3 has two operational modes: SAR mode and LRM. As the SAR mode is available globally, we are able to retrieve inland water levels over any area tracked by Sentinel-3.

The SRAL tracks the surface in two different tracking modes, namely, closed loop and open loop tracking (Figure 2). For closed loop tracking, the altimeter range window is autonomously positioned based on an on-board near real-time (NRT) analysis of the previous SRAL waveform; in contrast, for open loop tracking, the altimeter range window is positioned using a priori knowledge of the surface height stored in the instrument in a one-dimensional along-track DEM. The tracking modes for the studied water bodies over the Ebro River basin are listed in Table 2.

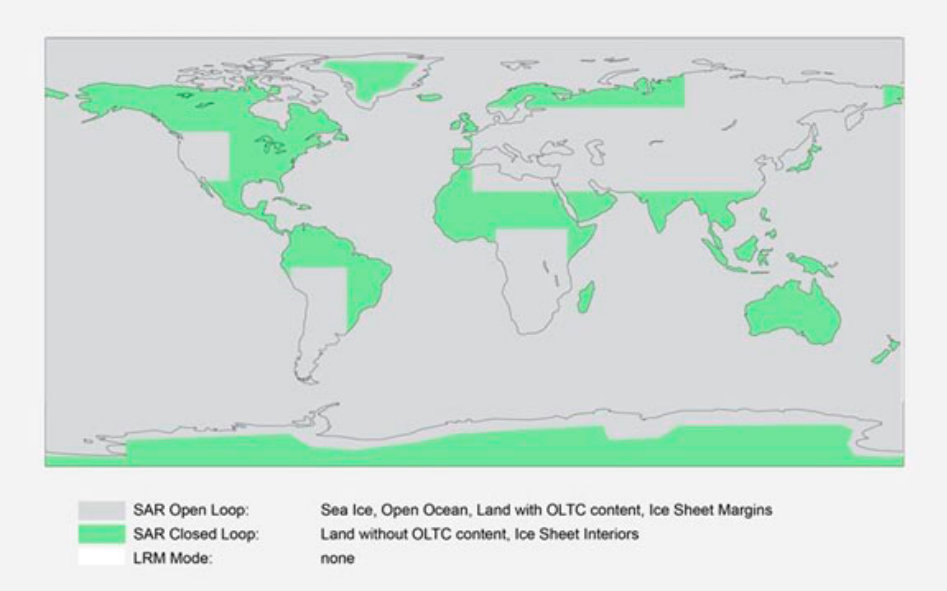

Figure 2. Sentinel-3 tracking modes (open loop and closed loop) per observed surface (Credit: ESA).

Three levels of processed altimeter data are available, namely, Level-0, Level-1 and Level-2 products. The Level-1 product is composed of data after instrumental corrections from the Level-0 product, which constitutes raw data. The Level-2 product is further processed by applying different retracking algorithms to the Level-1 waveforms to calculate the final altimeter range and the backscatter coefficient, including geophysical corrections. In our study, Level-1 data are used for the water level retrieval by the three retrackers (i.e., the threshold, OCOG and 2-step physical-based retrackers), while ESA Level-2 ocean retracked data are used for comparison.

The main objectives of the Level-2 processing of SAR mode data are to provide elementary retracked altimeter estimates of the oceans, coastal zones, ice sheets and sea ice elevations [27]. Different retracking algorithms are more suited to specific surfaces, that is, for ocean retracking, OCOG retracking, ice sheet retracking, ice retracking and sea ice retracking. Unfortunately, ice-related retracker results are not available for inland water bodies; hence, we used Level-2 ocean retracker results for comparison. Ocean retrackers try to fit theoretically modelled multi-look Level-1B (L1B) waveforms to real L1B SAR waveforms, thereby providing estimates of the epoch, composite sigma, amplitude and mispointing angle [27].

There are three different data product types: NRT, short-time critical (STC) and non-time critical (NTC) products. NRT data are delivered less than 3 hours after the data area acquired, whereas STC data are delivered within 48 hours, and NTC data are delivered within 1 month. The additional delay allows the consolidation of some auxiliary or ancillary data, including precise orbit data [26], which is important for inland water level retrieval. Therefore, we used NTC data to calculate the time series of inland water levels.

2.2.2. In situ data

In situ data for the Ebro River basin are available in the Automatic Hydrological Information System (SAIH) Ebro data hub [28]. SAIH Ebro is an online system providing hourly and daily hydrological information, including river gauge data, reservoir levels, rainfall amounts and temperatures, over the Ebro River basin. Together with the Sentinel-3 passes, we studied eight water bodies in our research, as listed in Table 2. The in situ data were collected from June 2016 to June 2018.

2.2.3. Digital elevation model

A DEM was used as an ancillary dataset for the selection of the waveform portion. The Shuttle Radar Topography Mission (SRTM) is an international research effort that obtains DEM data on a

near-global scale from 56°S to 60°N [29]. The SRTM provides global data at two resolutions: 1 arc-second (~30 m) and 3 arc-seconds (~90 m). In our study, 1 arc-second global elevation data, which offer a worldwide coverage of void-filled data at a resolution of approximately 30 m, are used.

3. Methodology

3.1. Principles of altimetry

The space-borne radar altimeter is an essential tool for monitoring the oceans, but it can also be used for inland water surfaces, including lakes and rivers. Space-borne radar altimeters transmit a short microwave pulse in the nadir direction, and the signal reflected by the surface is received by the instruments. The shape of the returned echo is what we call the waveform. The elapsed time corresponds to the range between the satellite and the Earth's surface [30]. The water level from an altimeter is derived from the measured range ($\boldsymbol{R}$), which is subtracted from the altitude of the satellite ($\boldsymbol{H_{alt}}$), after which different needed geophysical corrections are applied [31].

$$\begin{aligned} \boldsymbol{H_{waterlevel}} = \boldsymbol{H_{alt}} - \boldsymbol{R} \\ + \left(\boldsymbol{C_{dry_{tropo}}} + \boldsymbol{C_{wet_{tropo}}} + \boldsymbol{C_{iono}} + \boldsymbol{C_{solid_{earth_{tide}}}} + \boldsymbol{C_{pole_{tide}}} + \boldsymbol{C_{ocean_{tide}}}\right) \\ - \boldsymbol{C_{geoid}} \end{aligned} \quad (1)$$

In this study, corrections for the wet troposphere, dry troposphere, ionosphere, solid earth tide, geocentric pole tide and ocean loading tide are performed, and the geoid correction is applied. Since the Sentinel-3 Level-1 product does not include geophysical corrections, we extracted these values from the Level-2 product. The detailed corrections and their ranges are listed in Table 4 [32]. The Geoid model used is the Earth Gravitational Model 2008 (EGM2008) [33].

Table 4. Geophysical corrections from the Level-2 product

Correction	Model	Variable of Level-2 product	Range of correction
Dry troposphere	European Centre for Medium-Range Weather Forecasts (ECMWF) model [34]	Mod_dry_tropo_cor_meas_altitude_01	1.7-2.5 m
Wet troposphere	ECMWF model [34]	Mod_wet_tropo_cor_meas_altitude_01	0-50 cm
Ionosphere	Global Ionospheric Map (GIM) [35]	Iono_cor_gim_01_ku	6-12 cm
Solid earth tide	Cartwright model [36]	Solid_earth_tide_01	-30 to +30 cm
Geocentric polar tide	Historical pole location [37]	Pole_tide_01	-2 to +2 cm
Ocean loading tide	GOT00.2 model [38]	Ocean_tide_sol1_01	-2 to +2 cm

To improve the altimeter range accuracy, which is related to the water level measurement accuracy, the waveform needs to be retracked precisely to determine the accurate tracking point located on the leading edge (Figure 3) [39]. We tested three different retrackers, namely, the threshold, OCOG, and 2-step physical-based retrackers, to find the tracking points precisely from the land-contaminated waveforms.

Preprints (www.preprints.org) | NOT PEER-REVIEWED | Posted: 19 November 2018 doi:10.20944/preprints201811.0424.v1

Peer-reviewed version available at Remote Sensing 2019; doi:10.3390/rs11060718

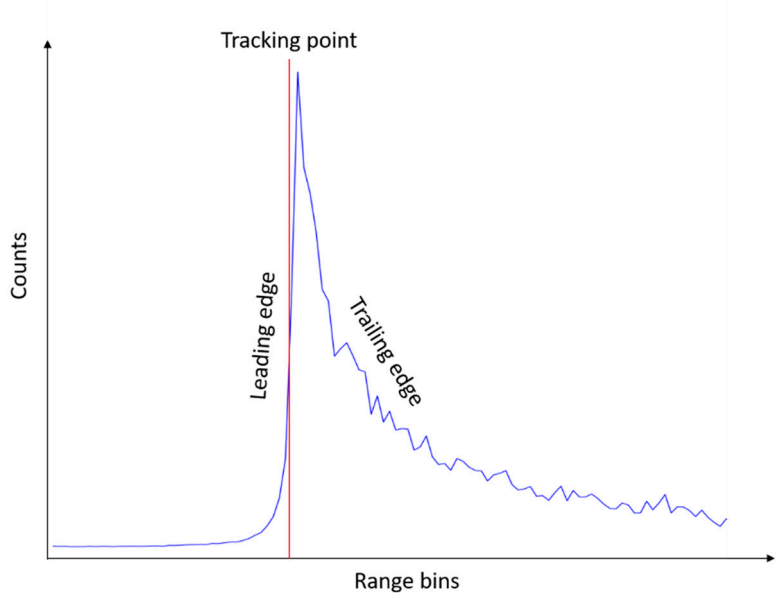

Figure 3. Re-tracking point illustration on the leading edge of the returned waveform.

3.2. Retrackers

3.2.1. Threshold retracker

The threshold retracker is a simple retracker based on an estimation of the epoch (the leading edge position) as a percentage of the maximum peak [40, 41]. In principle, it works well when the maximum peak originates from a nadir water body. The epoch is calculated as the first sample or range bin that is above a percentage of the waveform peak:

$$epoch = n_{th} - 1 + (A_{peak} \cdot \eta_{th} - y(n_{th} - 1))/(y(n_{th}) - y(n_{th} - 1)) \quad (2)$$

where n_{th} is the first range bin of the waveform right above the amplitude threshold ($A_{peak} \cdot n_{th}$), and A_{peak} is the amplitude of the peak of the waveform; η_{th} is defined as a threshold percentage of 50% in our case.

3.2.2. OCOG retracker

The OCOG retracker [42] was designed to calculate the centre of gravity of the reflected waveform based on the power levels in the bins. It is an empirical retracker that implements a combination of the centre of gravity (COG) and a conventional offset to estimate the related epoch (the leading edge position). Three main parameters are estimated for the OCOG retracker: the COG, the window size (W) and the amplitude (A).

Frappart's definition [43] is considered in our analysis using squares of the power samples:

$$COG = \frac{\sum_{n=n_1}^{n_2} n \cdot y^2(n)}{\sum_{n=n_1}^{n_2} y^2(n)}$$

$$W = \frac{\left(\sum_{n=n_1}^{n_2} y^2(n)\right)^2}{\sum_{n=n_1}^{n_2} y^4(n)} \quad (3)$$

$$A = \sqrt{\frac{\sum_{n=n_1}^{n_2} y^4(n)}{\sum_{n=n_1}^{n_2} y^2(n)}}$$

where y(n) is the n-th power sample of the input waveform, and n1 and n2 are the initial and end range bins or positions, respectively, in the waveform used for the OCOG parameter estimation.

Then, the estimated epoch can be implemented using the conventional OCOG definition of the epoch:

$$epoch = offset + (COG - W/2) \quad (4)$$

3.2.3. Two-step physical-based retracker

The 2-step physical-based retracker [44] is an in-house isardSAT implementation based on the SAR ocean model proposed by Chris Ray et al. [45], in which a physically based model of the SAR altimetric power waveform over the ocean is used to fit the backscattered signal received by the actual altimetric sensor. Details regarding the definition and implementation of this retracker can be found in the literature [44]. In SAR or delay-Doppler altimetry, different Doppler beams or looks are synthesized to focus on a given surface on the ground [43]; thus, the averaging of all these Doppler power beams will lead to the final multilook power waveform to be retracked. Therefore, for this physical-based retracker, each single-look power waveform needs to be modelled as follows:

$$\begin{aligned} P\_(k,l)\ (P\_u, epoch, SWH/MSS\ ) \\ = P\_u \cdot B\_(k,l)\ (MSS) \cdot \sqrt{(g\_l\ (SWH)\ )}\ [f\_0\ (g\_l\ (SWH) \cdot k) \\ + T\_(k,l)\ (MSS) \cdot g\_l\ (SWH) \cdot f\_1\ (g\_l\ (SWH) \cdot k)] \end{aligned} \quad (5)$$

where P_u is the amplitude, SWH is the significant wave height, and MSS is the mean square slope related to the surface roughness.

The original formulation is for open ocean scenarios, while the shape of the waveform reflected from an inland water body might exhibit more peaks (smoother surfaces) or ocean-like shapes (blowing winds over lakes). The retracker is therefore tuned to adapt to a variety of waveforms:

- SWH retracker: Fitting epoch, amplitude and SWH keeping the roughness parameter (MSS) fixed for ocean-like waveforms.
- MSS retracker: Fitting epoch, amplitude and MSS (roughness) keeping the SWH fixed for waveforms with more peaks.
- Two-step retracker: First fitting epoch, amplitude, and SWH keeping the roughness parameter fixed; if the correlation between the modelled waveform and measured waveform is below a given threshold, then a second run is performed by the fitting epoch, amplitude and roughness keeping the SWH fixed.

3.3. Selection of the waveform portion

Over inland water bodies, the on-board tracker might not properly locate the retrieval window to acquire the signal from the nadir corresponding to the water body; in addition, specific across-track surface contamination will be present in the waveforms, making it difficult to properly track the desired portion of the waveform. In our study, we use DEM information (SRTM DEM at a resolution of 30 m) to locate the waveform portion that comes from nadir within the retrieval window and then retrack the waveform using the selected portion only.

This method uses the window delay derived from the reference height beneath the satellite and is based on the DEM. It intrinsically uses a peak-valley approach: it selects the peak whose window delay is close to the nadir return and selects the samples defined by the valleys surrounding this peak in addition to some guard samples to the left and right.

3.4. Waveform filtering

For very small water bodies, the waveform may be highly contaminated by the land. Thus, additional conditions must be added to filter out the waveforms with a poor quality. We use three conditions to separate water-shaped waveforms from highly contaminated waveforms:

- Number of outstanding peaks < 5

- The epoch of the reference SRTM DEM must be within the waveform window
- Sigma_0 (backscatter coefficient) > 50 dB

First, within the vicinity of land, reflections from both water and land will contribute to the received waveform, resulting in more than one peak. If the number of outstanding peaks is larger than expected, the waveform may be contaminated substantially by land, making it difficult to distinguish water from land. Second, if the epoch of the reference SRTM DEM is outside the waveform window, whose measuring range is approximately 60 m, it is likely that the on-board tracker window was unable to focus on the reflecting surface. Finally, sigma_0, which is the backscatter coefficient for water from nadir, should be much larger than the backscatter coefficient for land. With these conditions, we can filter out waveforms that are unsuitable for detecting the levels of water bodies.

The workflow of the water level retrieval using the Level-1 product includes three main steps: selecting the waveform portion using a DEM, determining the retracking range using different retrackers, and filtering the waveforms, as shown in Figure 4. Geophysical corrections are applied to the retracked range using the Level-2 product, and the accuracy is assessed for each water body using in situ measurements from the gauging stations in the SAIH system.

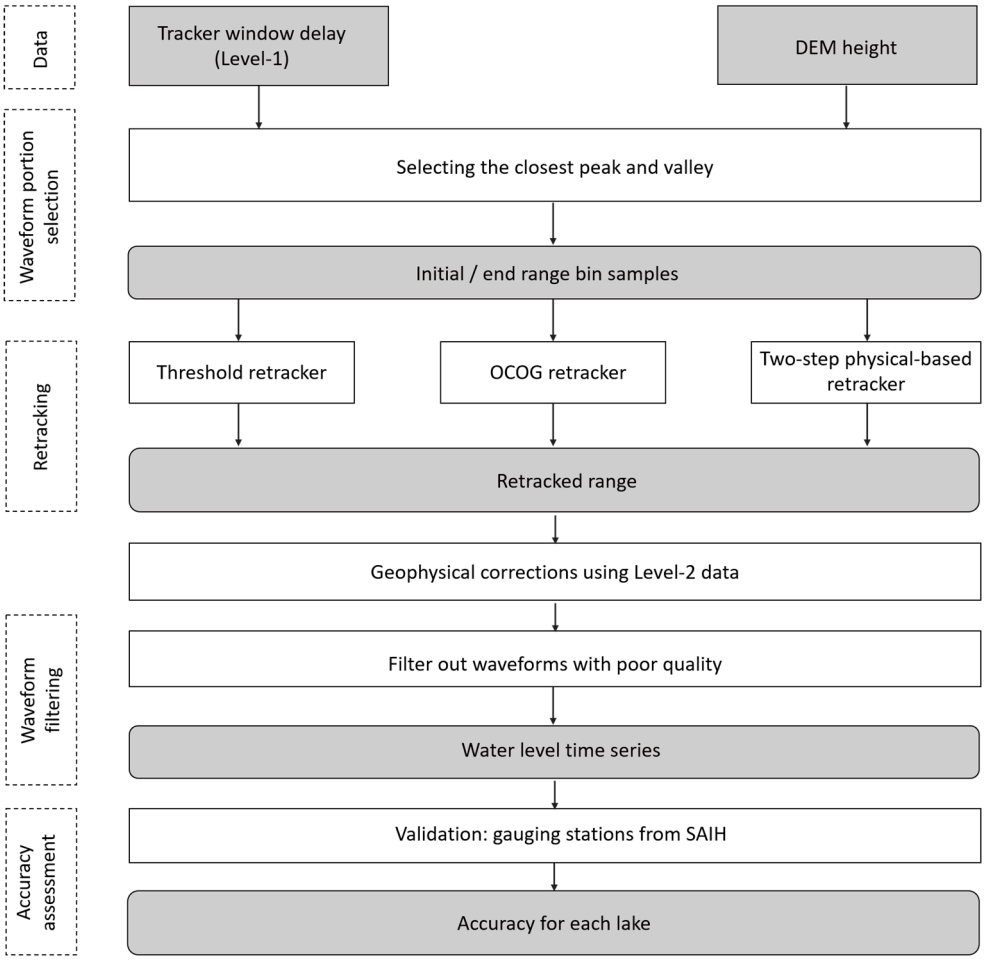

Figure 4. Overview of the workflow.

4. Results

4.1. Selecting the waveform portion using a DEM

When a waveform is influenced by land-based contamination, the waveform will contain small peaks due to off-nadir land or land coverage that follow the large peak, which corresponds to the reflection from the water surface. In this case, as shown in Figure 5, the portion of the selected

waveform provides a more precise tracking point for all three retrackers, especially for the OCOG retracker. The footprint of the signal is very close to the shore, thereby introducing a large peak at the trailing edge. The selection of the waveform portion uses the DEM information, the range bin of which is shown as a black vertical line in Figure 5, to find the closest peak and valley. For the 2-step physical-based retracker, the fitting using the selected waveform portion results in a 99% accuracy, while the fitting using the whole waveform results in an accuracy of 83%. For the OCOG retracker, the COG when using the selected waveform portion is located inside the first peak, while that when using the whole waveform is located in between peaks.

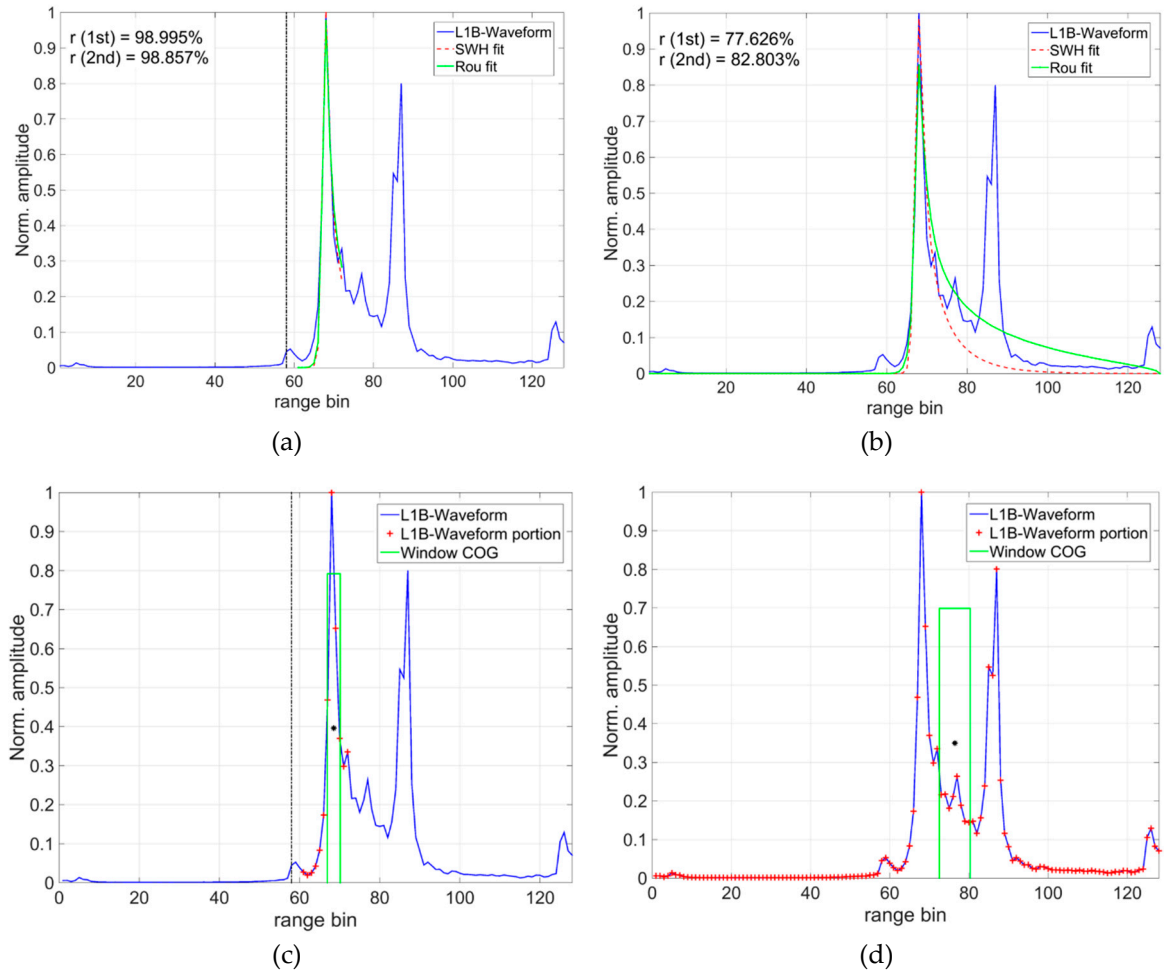

Figure 5. Comparison of the waveform portion selection method with the method using the whole waveform for the 2-step physical-based retracker and OCOG retracker: (a) 2-step physical-based retracker with the selected waveform portion; (b) 2-step physical-based retracker with the whole waveform; (c) OCOG retracker with the selected waveform portion; (d) OCOG retracker with the whole waveform.

The differences between the performance using the waveform portion selection method and the method using the whole waveform are also shown in the time series results over the Ebro Reservoir in Figure 6. The Level-2 data were obtained from the ESA Level-2 product using the ocean retracker without the waveform portion selection method. The waveform portion selection method eliminated most outliers compared with the method of using the whole waveform.

Preprints (www.preprints.org) | NOT PEER-REVIEWED | Posted: 19 November 2018 doi:10.20944/preprints201811.0424.v1

Peer-reviewed version available at Remote Sensing 2019; doi:10.3390/rs11060718

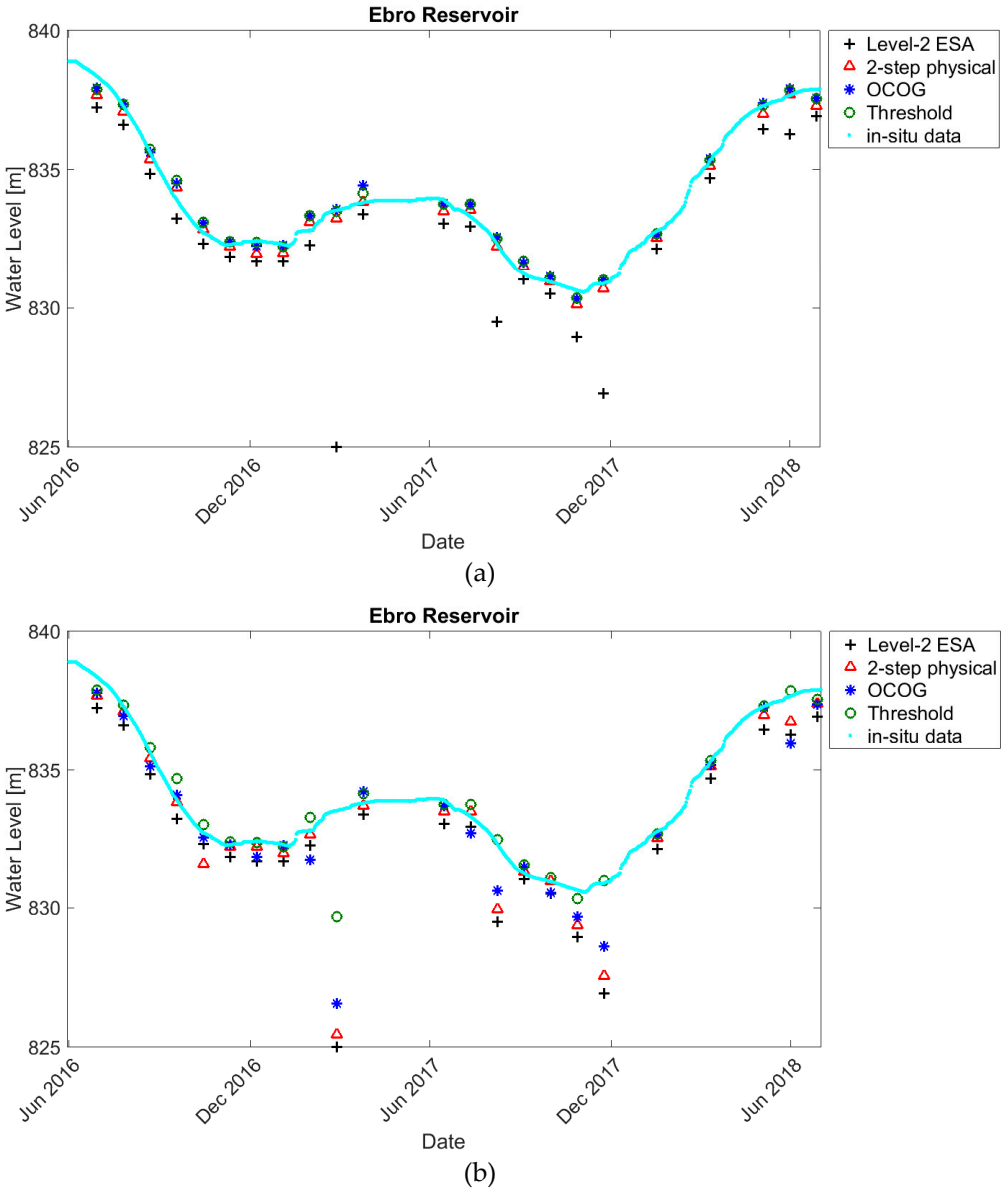

Figure 6. Time series water levels over the Ebro Reservoir using the waveform portion selection method (a) and using the whole waveform (b).

4.2. Time series validation

The time series of the water levels are calculated using a strict water mask polygon. The water levels of the altimeter footprints within the mask are considered, filtered and averaged for each date. Figure 6a and Figure 7 show the water levels for different water bodies derived using the three retrackers, namely, the 2-step physical-based retracker, OCOG retracker and threshold retracker, in combination with the waveform portion selection method. The retracked results are compared with the in situ measurements and the Level-2 results using the ocean retracker.

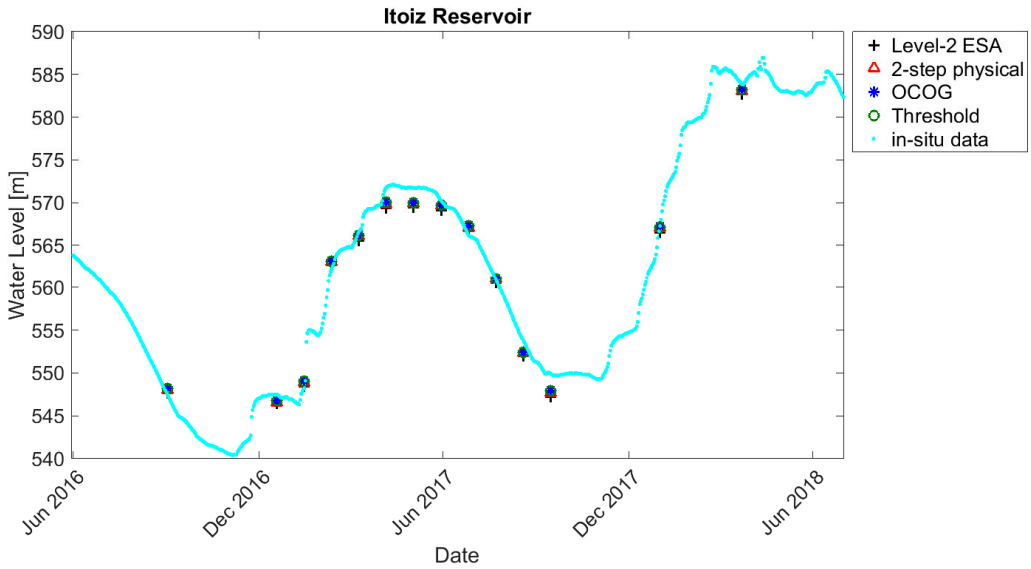

(a)

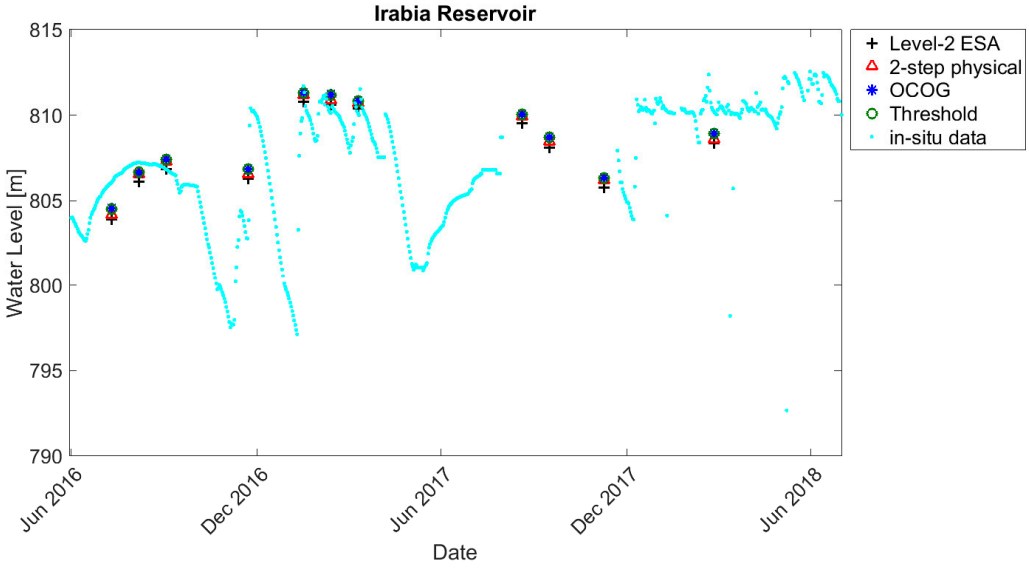

(b)

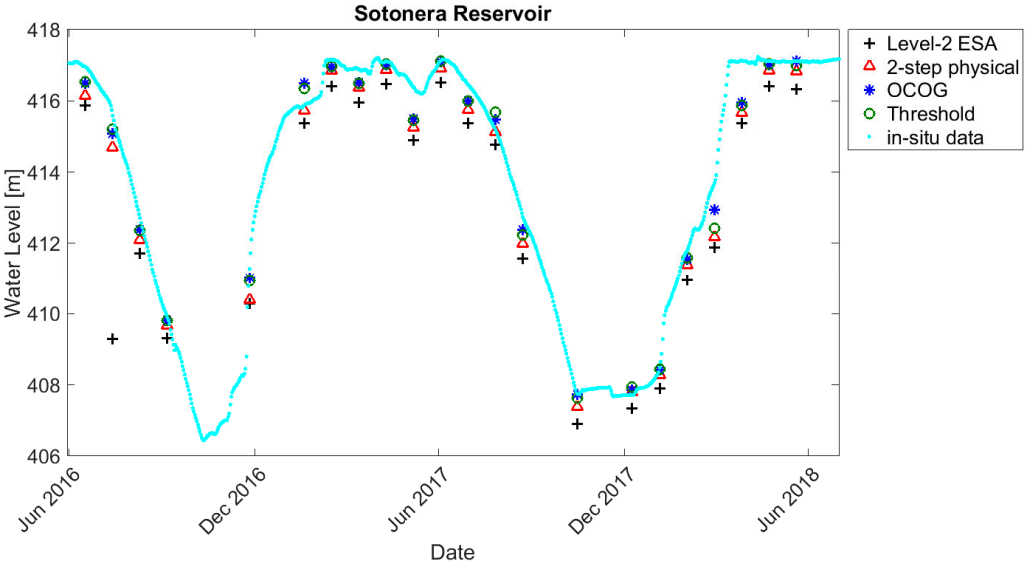

(c)

Preprints (www.preprints.org) | NOT PEER-REVIEWED | Posted: 19 November 2018 doi:10.20944/preprints201811.0424.v1

Peer-reviewed version available at Remote Sensing 2019; doi:10.3390/rs11060718

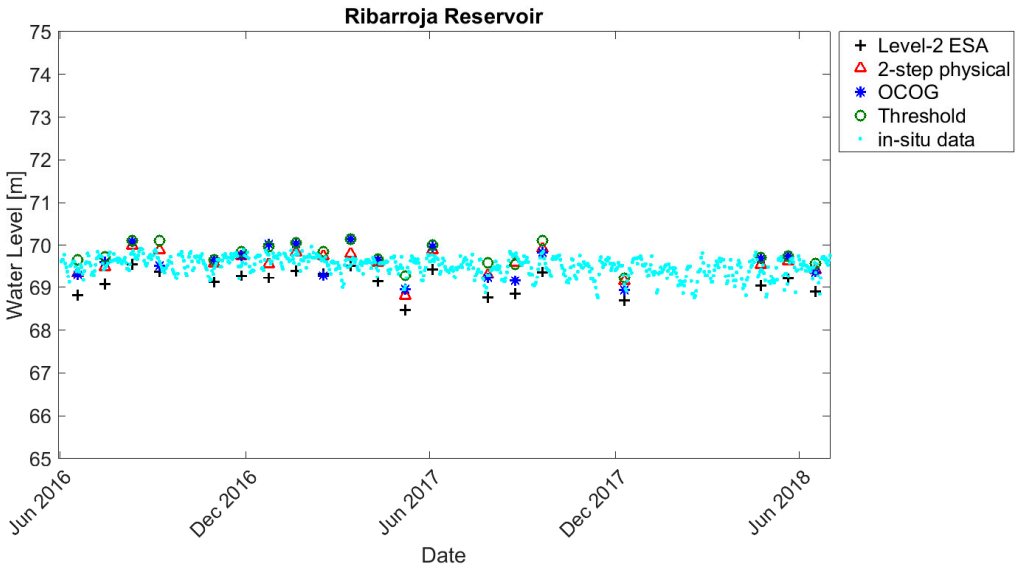

(d)

Figure 7. Water level time series over different water bodies: (a) Itoiz Reservoir; (b) Irabia Reservoir; (c) Sotonera Reservoir; (d) Ribarroja Reservoir.

Among the eight water bodies monitored in this study, the water levels over the Mequinenza Reservoir, Cavallers Reservoir and San Salvador Reservoir, all of which were tracked in an open loop tracking mode (on-board DEM dependent), could not be retracked. Figure 8 shows a comparison between the on-board tracking heights derived from the received waveforms and the heights from the SRTM DEM with reference to the geodetic ellipsoid. The difference between the two is almost 50 m over the Mequinenza Reservoir, more than 1000 m over the Cavallers Reservoir, and approximately 80 m over the San Salvador Reservoir. These findings indicate that the SRAL sensor lost its track and was unable to acquire the waveforms reflected from these water body surfaces.

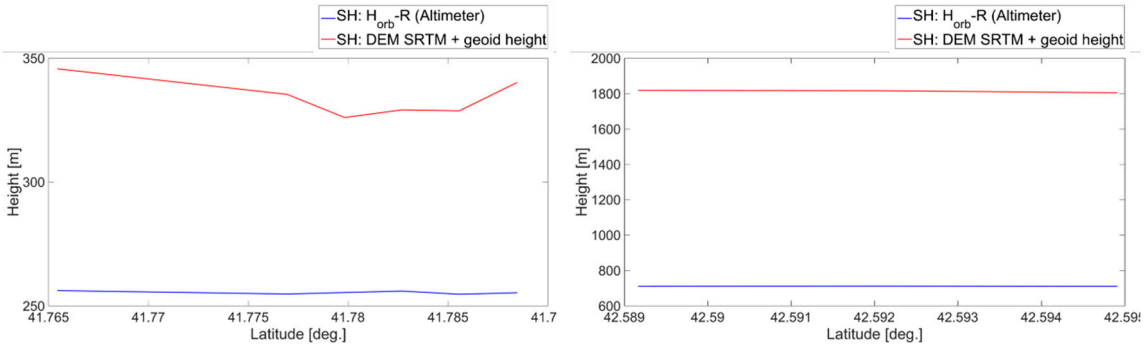

(a) (b)

Figure 8. Comparison of the retracked surface heights and the SRTM DEM surface heights (SH) with reference to the ellipsoid over the San Salvador Reservoir (a) and Cavallers Reservoir (b).

The RMSE and un-biased RMSE (ubRMSE) are calculated according to equations (6) and (7) and are listed in Table 5. The un-biased RMSE is more reliable because it removes the bias.

$$RMSE = \sqrt{E[(WL - insitu)^2]} \tag{6}$$

$$ubRMSE = \sqrt{E\{[(WL - E[WL]) - (insitu - E[insitu])]^2\}} \tag{7}$$

where E[·] is the expectation operator and WL is the water level derived from satellite data. The RMSEs for different water bodies vary from 17 cm to more than 1 m. A comparison of the performances for the different retrackers over different water bodies is shown in Table 5. The best result is obtained for the Ribarroja Reservoir, which has an ubRMSE of approximately 16 cm. The

results over the Ebro Reservoir, Sotonera and Ribarroja Reservoirs are also satisfactory. The RMSEs for the Itoiz Reservoir and Irabia Reservoir are relatively large with values greater than 1 m. The results using the three different retrackers do not show large differences except for the Sotonera Reservoir and Ribarroja Reservoir. The OCOG retracker gives the smallest ubRMSE for the Sotonera Reservoir with a value of approximately 38 cm. The 2-step physical-based retracker and threshold retracker work better over the Ribarroja Reservoir than the OCOG retracker, which has an ubRMSE of approximately 16 cm. All of the retrackers give better results than the Level-2 ocean retracker without the waveform portion selection method.

Table 5. Comparison of the water level validation results over all monitored water bodies

Water bodies	Width	Tracking mode	RMSE / ubRMSE [m]			
			Two-step physical	OCOG	Threshold	Level-2 ocean
Ebro Reservoir	1.8 km	Closed loop	0.32 / 0.29	0.30 / 0.28	0.30 / 0.28	2.18 / 1.76
Itoiz Reservoir	400 m-2.7 km	Closed loop	1.18 / 1.02	1.10 / 1.00	1.10 / 1.00	1.41 / 1.03
Irabia Reservoir	130 m	Closed loop	1.39 / 1.39	1.39 / 1.38	1.39 / 1.38	1.44 / 1.39
Sotonera Reservoir	4.5 km	Closed loop	0.60 / 0.43	0.49 / 0.38	0.48 / 0.44	1.65 / 1.19
Ribarroja Reservoir	400 m	Open loop	0.18 / 0.16	0.29 / 0.28	0.31 / 0.16	0.44 / 0.20
Mequinenza Reservoir	600 m	Open loop	Off-track			
Cavallers Reservoir	800 m	Open loop	Off-track			
San Salvador Reservoir	1.2 km	Open loop	Off-track			

5. Discussion

The water levels of all water bodies tracked in closed loop mode can be tracked, while three water bodies are missed in open loop mode, and only one is tracked accurately. The results over the Ebro Reservoir, Sotonera and Ribarroja Reservoirs are satisfactory. The Ebro Reservoir is located in the north near the Pyrenees mountain range with elevations exceeding 820 m. The RMSE is 30 cm compared with the in situ measurements. The Sotonera and Ribarroja Reservoirs are located in relatively flat areas, and the results are good because there is no influence from the mountainous terrain. The RMSEs over the Itoiz Reservoir and Irabia Reservoir exceeds 1 m. One reason for this could be the rapid change in the elevations along the satellite track because both water bodies are located in the Pyrenees, which makes it easy for a satellite to lose its track. The width of the Itoiz Reservoir with satellite data varies from 400 m to more than 2 km depending on the different satellite tracks, which drift on a daily basis. In addition, the Irabia Reservoir is a very small water body whose width is only approximately 130 m, making the retrieval of its surface height more challenging.

The results of the three retrackers, namely, the 2-step physical-based retracker, OCOG retracker and threshold retracker, in combination with the waveform portion selection method are always better than the results of the Level-2 ocean retracker; the results of both sets of retrackers are shown in Figure 5 and Figure 6. Therefore, given the lack of an ice retracker over inland water bodies, retrieving the water levels by retracking the Level-1 waveforms and using the waveform portion selection method constitutes an alternative approach to retrieving more accurate water levels.

The open loop tracking mode was not capable of monitoring the water levels in the Mequinenza Reservoir, Cavallers Reservoir and San Salvador Reservoir. The DEM resolution of the Sentinel-3 SRAL needs to be updated to be capable of monitoring more inland bodies; alternatively, the tracking mode needs to be switched to the closed loop mode.

The different retrackers obtained a good accuracy with in situ measurements. Errors in the in situ data might be related to the drift of the river course (the measurements are not co-located with the Sentinel-3 track) or the waveform quality, which depends on the surrounding terrain, because the geometry of the lake shore and the characteristics of the terrain all contribute to the shape of the waveform. Nevertheless, Sentinel-3 has been proven to work for small water bodies.

6. Conclusions

The study compared the performances of the threshold, OCOG and 2-step physical-based retrackers in combination with a novel waveform portion selection approach over inland water bodies. In this paper, the water levels are compared with in situ measurements and the ESA Level-2 ocean retracker. The results show good agreement with the in situ measurements. The ubRMSE over the Ribarroja Reservoir can reach 16 cm, while that over the Ebro Reservoir can reach 28 cm. In contrast, the accuracy over water bodies located in mountainous areas still needs to be improved, but the results demonstrate the possibility of retrieving the water levels over a very small water body with a width of approximately 130 m.

The DEM-oriented waveform portion selection method is fairly able to isolate the nadir peak from land-based contamination. Retracking the water levels from Level-1 waveforms using the combination of a retracker and the waveform portion selection method is more robust to land contamination than using Sentinel-3 Level-2 data directly and results in a better accuracy.

We have detected some issues related to the Sentinel-3 SRAL tracking mode. The open loop tracking mode, which depends on the on-board DEM to locate the tracking window, loses its track over the Cavallers Reservoir, which is surrounded by mountains, in addition to the Mequinenza and San Salvador Reservoirs, which are in relatively flat areas. Improvements need to be applied to the altimeter's performance either by updating the on-board DEM with a better resolution over water bodies of interest or by changing the tracking mode to a closed loop mode.

Overall, the Sentinel-3 SRAL has been proven to work over inland water bodies, even those with widths as small as 130 m. Retracking using the 2-step physical-based retracker, OCOG retracker and threshold retracker with the waveform portion selection method using an SRTM DEM improves the accuracy with an optimal ubRMSE of 16 cm. Further steps need to be taken to explore the possibilities both for tracking water bodies that are not currently being tracked and for improving the accuracies for very small water bodies with Sentinel-3 altimeter data.

Author Contributions: Q.G., E.M. and M.J.E. conceived, designed and implemented the research. Q.G. and E.M. coded the program. Q.G. performed the analysis of the data and drafted the manuscript. M.J.E. assisted in the data analysis and interpretation. All authors reviewed and improved the manuscript. The study was supervised by M.J.E.

Funding: Qi Gao received grant DI-15-08105 from the Spanish Education Ministry (MICINN) and DI-2016-078 from the Catalan Agency of Research (AGAUR). This work has been partially funded by the Spanish Ministry of Science, Innovation and Universities and the European Regional Development Fund through grant CGL2017-85687-R.

Acknowledgements: The authors wish to thank the technical teams for their support, the Copernicus Programme, which provided open access to the Sentinel data, and the SAIH Ebro team, who provided the ground information.

Conflicts of Interest: The authors declare no conflicts of interest.

References

1. Benveniste, J. Radar Altimetry: Past, Present and Future. In *Coastal Altimetry*, Vignudelli, S.; Kostianoy, A.; Cipollini, P.; Benveniste J. Springer: Berlin, Heidelberg, 2011; ISBN: 978-3-642-12795-3. DOI: 10.1007/978-3-642-12796-0_1.
2. Alsdorf, D. E.; Rodriguez, E.; Lettenmaier, D. P. Measuring surface water from space. *Reviews of Geophysics*, **2007**, 45(2), RG2002, DOI: 10.1029/2006RG000197.
3. Calman, S.; Seyler, F. Continental surface water from satellite altimetry. *Comptes Rendus Geosciences*, **2006**, 338(14–15), 1113–1122, DOI: 10.1016/j.crte.2006.05.012.
4. Cretaux, J. F.; Birkett, C. Lake studies from satellite radar altimetry. *Comptes Rendus Geosciences*, **2006**, 338,1098–1112, DOI: 10.1016/j.crte.2006.08.002.
5. Raney, R.K. The delay/Doppler radar altimeter. *IEEE Transactions on Geoscience and Remote Sensing*, **1998**, 36, 1578-1588, DOI: 10.1109/36.718861.
6. Koblinsky, C.J.; Clarke, R.T.; Brenner, A.C.; Frey, H. Measurement of river level variations with satellite altimetry. *Water Resour. Res*. **1993**, 29, 1839–1848. DOI: 10.1029/93WR00542.
7. Birkett, C. The contribution of TOPEX/POSEIDON to the global monitoring of climatically sensitive lakes. *J. Geophys. Res. – Oceans*, **1995**, 100, 25179–25204. DOI: 10.1029/95JC02125.
8. Birkett, C.M. Contribution of the TOPEX NASA radar altimeter to the global monitoring of large rivers and wetlands. *Water Resour. Res*. **1998**, 34, 1223–1239. DOI: 10.1029/98WR00124.
9. Jarihani, A.A.; Callow, J.N.; Johansen, K.; Gouweleeuw, B. Evaluation of multiple satellite altimetry data for studying inland water bodies and river floods. *J. Hydrol*. **2013**, 505, 78–90. DOI: 10.1016/j.jhydrol.2013.09.010.
10. Yi, Y.; Kouraev, A.V.; Shum, C.K.; Vuglinsky, V.S.; Cretaux, J.F.; Calmant, S. The performance of altimeter waveform retrackers at Lake Baikal. *Terr. Atmos. Ocean. Sci*. **2013**, 24, 513–519. DOI: 10.3319/TAO.2012.10.09.01(TibXS).
11. Nielsen, K.; Stenseng, L.; Andersen, O.B.; Villadsen, H.; Knudsen, P. Validation of CryoSat-2 SAR mode based lake levels. *Remote Sens. Environ*. **2015**, 171, 162–170. DOI: 10.1016/j.rse.2015.10.023.
12. Schwatke, C.; Dettmering, D.; Boergens, E.; Bosch, W. Potential of SARAL/AltiKa for inland water applications. *Mar. Geodesy*. **2015,** 38, 626–643. DOI: 10.1080/01490419.2015.1008710.
13. Villadsen, H.; Andersen, O.; Stenseng, L.; Nielsen, K.; Knudsen, P. CryoSat-2 altimetry for river level monitoring – evaluation in the Ganges-Brahmaputra River basin. *Remote Sens. Environ*. **2015**, 168, 80–89. DOI: 10.1016/j.rse.2015.05.025.
14. Schwatke, C.; Dettmering, D.; Bosch, W.; Seitz, F. DAHITI - an innovative approach for estimating water level time series over inland waters using multi-mission satellite altimetry. *Hydrol. Earth Syst. Sci.*, **2015**, 19, 4345-4364, DOI: 10.5194/hess-19-4345-2015.
15. Wheeler, J.; Berry, P.A.M.; Smith, R.G.; Benveniste, J. The ESA Near Real Time River and Lake System. The Proceedings of the Earth Observation and Water Cycle Science; 18th-20th November, 2009, ESA ESRIN, Frascati, Italy; ISBN 978-92-9221-238-4
16. Crétaux, J.-F.; Jelinski, W.; Calmant, S.; Kouraev, A.; Vuglinski, V.; Bergé-Nguyen, M.; Gennero, M.-C.; Nino, F.; Abarca Del Rio, R.; Cazenave, A.; Maisongrande, P., SOLS: A Lake database to monitor in Near Real Time water level and storage variations from remote sensing data, *J. Adv. Space Res*. **2011**, 47, 1497-1507, DOI:10.1016/j.asr.2011.01.004.
17. Birkett, C.M.; Reynolds, C.; Beckley, B.; Doorn, B. From Research to Operations: The USDA Global Reservoir and Lake Monitor, chapter 2 in Coastal Altimetry, Springer Publications, Vignudelli, S.; Kostianoy, A.G.; Cipollini, P.; Benveniste, J. 2010, ISBN 978-3-642-12795-3.
18. Gustafsson,D.; Andersson, J.; Brito, F.; Martinez, B.; Arheimer, B. New tool to share data and models in hydrological forecasting, based on the ESA TEP. Proceedings of EGU 2018 symposium, Vienna, Austria, 8–13 April 2018.
19. Birkinshaw, S.J.; O'Donnell, G.M.; Moore, P.; Kilsby, C.G.; Fowler, H.J.; Berry, P.A.M. Using satellite altimetry data to augment flow estimation techniques on the Mekong River. *Hydrol. Process*. **2010**, 24, 3811–3825. DOI: 10.1002/hyp.7811.
20. da Silva, J.S.; Calmant, S.; Seyler, F.; Rotunno Filho, O.C.; Cochonneau, G.; Mansur, W. J. Water levels in the Amazon basin derived from the ERS 2 and ENVISAT radar altimetry missions. *Remote Sens. Environ.* **2010**, 114, 2160–2181. DOI: 10.1016/j.rse.2010.04.020.

21. Michailovsky, C.I.; McEnnis, S.; Berry, P.A.M.; Smith, R.; Bauer-Gottwein, P. River monitoring from satellite radar altimetry in the Zambezi River Basin. *Hydrol. Earth Syst. Sci.* **2012**, 9, 3203–3235. DOI: 10.5194/hess-16-2181-2012.
22. Maillard, P.; Bercher, N.; Calmant, S. New processing approaches on the retrieval of water levels in Envisat and SARAL radar altimetry over rivers: a case study of the Sao Francisco River, Brazil. *Remote Sens. Environ.* **2015**, 156, 226–241. DOI: 10.1016/j.rse.2014.09.027.
23. Boergens, E.; Nielsen, K.; Andersen, O.B.; Dettmering, D.; Seitz, F. River Levels Derived with CryoSat-2 SAR Data Classification—A Case Study in the Mekong River Basin. *Remote Sens.* **2017**, 9, 1238. DOI: 10.3390/rs9121238.
24. Cretaux, J.-F.; Calmant, S. Spatial Altimetry and Continental Waters, In Land Surface Remote Sensing in Continental Hydrology. Baghdadi, N.; Zribi, M. Elsevier, **2016**; https://doi.org/10.1016/B978-1-78548-104-8.50006-1.
25. Ebro. In Wikipedia, The Free Encyclopedia. Available online: https://en.wikipedia.org/w/index.php?title=Ebro&oldid=862269870 (accessed on 3 October 2018)
26. Sentinel-3 Team. Sentinel-3 User Handbook. European Space Agency. Available online: https://earth.esa.int/documents/247904/685236/Sentinel-3_User_Handbook-iss1_v1_20170113/960ff616-87f5-43cc-b23e-3e96030bd13a (accessed on 15 March 2018).
27. Re-Tracking Estimates. Available online: https://sentinel.esa.int/web/sentinel/technical-guides/sentinel-3-altimetry/level-2/re-tracking-estimates (accessed on 3 October 2018).
28. SAIH Ebro. http://www.saihebro.com.
29. Farr, T.G.; Rosen, P.A.; Caro, E.; Crippen, R.; Duren, R.; Hensley, S.; Kobrick, M.; Paller, M.; Rodriguez, E.; Roth, L.; Seal, D.; Shaffer, S.; Shimada, J.; Umland, J.; Werner, M.; Oskin, M.; Burbank, D.; Alsdorf, D. The Shuttle Radar Topography Mission. *Reviews of Geophysics*. **2007**, 45 (2), DOI: 10.1029/2005RG000183.
30. Calmant, S.; Seyler, F.; and Cretaux, J.F. Monitoring continental surface waters by satellite altimetry. *Surveys in Geophysics*, **2008**, 29, 247–269, DOI: 10.1007 / s10712-008-9051-1.
31. Fernandes, M.J.; Lázaro, C.; Nunes, A.L.; Scharroo, R. Atmospheric Corrections for Altimetry Studies over Inland Water. *Remote Sens.* **2014**, 6, 4952-4997. DOI: 10.3390/rs6064952.
32. Sentinel-3A L2P SLA Product Handbook. Available online: https://www.aviso.altimetry.fr/fileadmin/documents/data/tools/hdbk_L2P_S3.pdf (accessed on 1 November 2017)
33. Pavlis, N. K.; Holmes, S. A.; Kenyon, S. C.; Factor, J. K. The development and evaluation of the Earth Gravitational Model 2008 (EGM2008). *Journal of Geophysical Research: Solid Earth*. **2012**, 117, B4. DOI: 10.1029/2011JB008916
34. Boehm, J.; Kouba, J.; Schuh, H. Forecast Vienna Mapping Functions 1 for real-time analysis of space geodetic observations. *J Geod*, **2009**, 83: 397. DOI: 10.1007/s00190-008-0216-y.
35. Scharroo, R.; Smith, W.H.F. Global positioning system-based climatology for the total electron content in the ionosphere. *J. Geophys. Res.* **2010**, 115. DOI: 10.1029/2009JA014719.
36. Cartwright, D.E.; Edden, A.C. Corrected Tables of Tidal Harmonics. *Geophysical Journal International*, **1973**, 33 (3), 253–264, DOI: 10.1111/j.1365-246X.1973.tb03420.x.
37. Wahr, J.M. Deformation of the Earth induced by polar motion. *J. Geophys. Res. (Solid Earth)*, **1985**, 90, 9363-9368. DOI: 10.1029/JB090iB11p09363.
38. Ray, R.D.; Ponte, R.M. Barometric tides from ECMWF operational analyses, *Annales Geophysicae*, **2003**, 21, 1897-1910. DOI: 10.5194/angeo-21-1897-2003.
39. Deng, X.; Featherstone, W.E. A coastal retracking system for satellite radar altimeter waveforms: Application to ERS-2 around Australia. *JOURNAL OF GEOPHYSICAL RESEARCH*, **2006**, vol. 11. DOI: 10.1029/2005JC003039.
40. Davis, C.H. Growth of the Greenland ice sheet: a performance assessment of altimeter retracking algorithms. *IEEE Trans Geosci Remote Sens*. **1995**, 33(5):1108–1116, DOI: 10.1109/36.469474.
41. Davis, C.H. A robust threshold retracking algorithm for measuring ice-sheet surface elevation change from satellite radar altimeter. *IEEE Trans Geosci Remote Sensing*. **1997**, 35(4): 974–979, DOI: 10.1109/36.602540.
42. Wingham, D.J.; Rapley, C.G., Griffiths, H. New techniques in satellite tracking system. In: Proceedings of IGARSS' 86 symposium, Zurich, 1986, pp 1339–1344

43. Frappart, F.; Calmant, S.; Cauhopé, M.; Seyler, F.; Cazenave, A. Preliminary results of ENVISAT RA-2-derived water levels validation over the Amazon basin. *Remote sensing of Environment,* **2006**, 100, 252-264. DOI: 10.1016/j.rse.2005.10.027.
44. Makhoul, E.; Roca, M.; Ray, C.; Escolà, R.; Garcia-Mondéjar, A. Evaluation of the precision of different Delay-Doppler Processor (DDP) algorithms using CryoSat-2 data over open ocean. *Advances in Space Research* **2018**, 62, 1464-1478. DOI: 10.1016/j.asr.2018.04.004.
45. Ray, C.; Martin-Puig, C.; Clarizia, M.P.; Ruffini, G.; Dinardo, S.; Gommenginger, C.; Benveniste, J. SAR altimeter backscattered waveform model, *IEEE Trans. Geosci. Remote Sens*., **2015**, 53, 911-919, DOI: 10.1109/TGRS.2014.2330423.